EUROPEAN ORGANIZATION FOR NUCLEAR RESEARCH

CERN-PPE/91-03
16 January 1991

INTERACTIONS OF 200 GeV/NUCLEON ^{16}O AND ^{32}S IONS IN NUCLEAR EMULSIONS

G. Baroni[h], V. Bisi[j], A.C. Breslin[c], D.H. Davis[f], S. Di Liberto[h], G. Grella[i], P. Giubellino[j], K. Hoshino[g], M. Kazuno[d], K. Kodama[e], Y. Maeda[k], A. Marzari-Chiesa[j], M.A. Mazzoni[b], F. Meddi[h], M.T. Muciaccia[a],K. Niu[g], L. Ramello[j], L. Riccati[j], G. Romano[i], G. Rosa[h], C. Sgarbi[h], H. Shibuya[d], S. Simone[a], D.N. Tovee[f], T. Virgili[h], C. Wilkin[f] and S.K.C. Yuen[f]

ABSTRACT

This paper presents and contrasts features of the inelastic nuclear reactions of 200 GeV/nucleon ^{16}O and ^{32}S ions with emulsion nuclei. Both the multiplicities of shower particles and the extent of target fragmentation have been studied for varying degrees of disruption of the projectile nuclei. The results may be interpreted within a simple geometrical model. In particular the rapidity distributions of those events which exhibit complete projectile break-up without any overt sign of low energy target fragmentation have been determined. The interaction of secondary projectile fragments of charge two or more issuing from oxygen interactions were also studied and the mean free paths in emulsion of the primary ^{16}O and ^{32}S ions and all such fragments have been compared to those predicted by a simple Glauber model.

Submitted to Nuclear Physics A

[a] Dipartimento di Fisica dell' Università and INFN, Bari, Italy.
[b] CERN, Geneva, Switzerland.
[c] Department of Physics, University College, Dublin, Ireland.
[d] Department of Physics, Toho University, Funabashi, Japan.
[e] Aichi University of Education, Kariya, Japan.
[f] Department of Physics & Astronomy, University College London, London, UK.
[g] Department of Physics, Nagoya University, Nagoya, Japan.
[h] Dipartimento di Fisica, Università 'La Sapienza' and INFN, Rome, Italy.
[i] Dipartimento di Fisica Teorica e SMSA dell' Università and INFN, Salerno, Italy.
[j] Dipartimento di Fisica dell' Università and INFN, Turin, Italy.
[k] Faculty of Education, Yokohama National University, Yokohama, Japan.

1. INTRODUCTION

As part of a large effort to find evidence for the formation of the elusive quark–gluon plasma states, emulsion, stacks were exposed to high energy ^{16}O and ^{32}S ions upstream of the HELIOS apparatus [1]. In this quest, interactions occurring within the emulsion, which subsequently display high transverse energy or high multiplicity in the downstream electronic detection system, have been selected for careful scrutiny in order to isolate features which, might indicate quark–gluon plasma formation [2]. However, for such a programme to be realizable, it is necessary to establish well the characteristics to be expected of 'normal' heavy ion–emulsion nucleus collisions. With this in mind, a study of sizeable and unbiased samples of the interactions of 200 GeV/nucleon ^{16}O and ^{32}S ions with emulsion nuclei has been carried out. Preliminary results on a subsample of ^{16}O interactions have already been published [3].

2. EXPERIMENTAL PROCEDURE

Emulsion pellicles of 600 μm thickness were prepared at CERN from Fuji ET 7B gel just prior to exposure. This procedure was carried out in an atmosphere of 70% relative humidity and the resulting emulsions were found to have a density of $(3.60 \pm 0.01) \times 10^3$ kg m^{-3}, which is some 6% less than the so-called 'standard' one [4]. On the assumption that the disparity in the density is solely due to an increase in the water content of the present emulsion, the elemental abundances have been calculated for the major constituents and these are compared to those of 'standard' emulsion in Table 1.

Having been poured, dried and peeled from their glass backing, the emulsions were guillotined to produce pellicles of the desired dimensions, 160 mm $\times$ 50 mm $\times$ 600 μm. These were then assembled into stacks and two, each of 62 pellicles, were exposed to the 200 GeV/nucleon ^{16}O beam in the West Area at CERN in December 1986 and four, each of 60 pellicles, were exposed to the 200 GeV/nucleon ^{32}S beam in November 1987. In all the exposures the beam was parallel to the longer side and horizontal with respect to the pellicle surfaces.

In order to reduce the bias against detecting small 'stars', the search for interactions was carried out using a line-scanning technique. In this, tracks of beam particles were located 10 mm from the entrance edge of the emulsion stack and those within the central 80% of the pellicle thickness were followed for a distance of 30 mm or until an interaction point was reached. However, since some interactions, particularly those ascribed to the electromagnetic dissociation of the projectile nucleus, are not discernable at the interaction vertex but only become apparent further downstream, tracks were followed for an additional 10 to 20 mm solely to detect such interactions occurring within the fiducial region. The interaction points were noted and the following features of each interaction were recorded: the number N_b of black tracks (if of protons, of kinetic energy < 30 MeV) and the number N_g of grey tracks (corresponding to protons in the energy range 30 to ~ 300 MeV) in the forward and backward hemispheres, the presence of doubly and multiply charged fragments of the projectile nucleus proceeding from the interaction essentially undeviated from the original beam direction and the approximate numbers of near-minimum ionizing (shower) particles. In order to avoid the inclusion of the many instances of fast δ-ray or low energy pair production in the sample, all events exhibiting solely one or two wide angle (> 5 mrad to the beam particle) minimum ionizing particles were rejected. As a consequence, nuclear interactions which present such topologies have also been removed from the sample.

Events in which all that is observed is the low energy break-up of the projectile nucleus have been ascribed to electromagnetic dissociation processes. Events which exhibit no shower particles, one low energy 'proton', with the projectile ion emerging essentially undeviated, have been noted. These are due in part to elastic collisions on free protons in the emulsion and also to the electromagnetic dissociation of the target nuclei. However the scanning efficiency for such events is too low for meaningful estimates of the corresponding cross sections to be made and they have thus not been considered further.

In a sample of the oxygen events the tracks of forward-going projectile fragments of charge greater than one—it being assumed that they retain the original 200 GeV/c per nucleon beam momentum—were subjected to the following analysis. The charge of the fragment was determined from grain density (helium) and δ-ray density (heavier ions) measurements, the charge resolution achieved from δ-ray measurements being shown in Fig. 1. The track was then followed for a distance of 60 mm or until an interaction point was reached, the following being extended for a further 10 mm beyond the fiducial region for the reasons already stated. The same features of secondary interactions were recorded as for primary ones and once again forward-going projectile fragments had their charges ascertained and were followed a further 60 mm or until they interacted. This procedure was repeated until any remaining forward-going fragments had gone 60 mm or they had left the pellicles. The establishment of the fragment charges in this way also enabled the primary oxygen interactions to be examined in greater detail.

3. RESULTS

3.1 Mean Free Paths

The results of the following of both the primary ^{16}O and ^{32}S ions as well as the subsequent investigation of secondary (+ tertiary ...) projectile fragments from oxygen interactions are summarized in Table 2. The analysis and discussion of events ascribed to electromagnetic dissociation are presented elsewhere [5]. The mean free path for 200 GeV/nucleon ^{16}O ions determined here, 120 $\pm$ 2 mm, is in accord with values found by other workers at this energy, *viz.* 119 $\pm$ 4 mm [6], 120 $\pm$ 3 mm [7] and 115 $\pm$ 6 mm [8] although emulsions with slightly different compositions were used in the other experiments, which should decrease their path lengths by about 3%. On the other hand the mean free path for ^{32}S ions, 92 $\pm$ 2 mm is much shorter than the other reported value of 111 $\pm$ 3.5 mm [8]; the difference in emulsions should produce an effect in the opposite direction. Any systematic errors due to scanning efficiency would tend to increase the mean free path and it is reassuring that the variation in our result from ^{16}O to ^{32}S is in accord with the optical model calculation reported below. The mean free path for He isotopes, 228 $\pm$ 11 mm, is consistent with that found for He projectile fragments from 200 GeV/nucleon ^{32}S ions [9] and 60 GeV/nucleon ^{16}O ions [10] when account is taken of the different emulsion composition. It is however higher than the result for 12 GeV/nucleon α-particles of 181 $\pm$ 7 mm [11] and it seems unlikely that this discrepancy can be explained wholly by the presence of ^{3}He fragments in our sample, the energy variation of the cross sections and the different emulsion conditions.

When determining the mean free paths of secondary fragments of various charges, both the interactions and the track length occurring within 2 mm of the primary vertex have been discarded. This cut has been made for two reasons. A track length of at least this distance is necessary to obtain an adequate determination of the charge of the fragment

from δ-ray counting. In addition, in the vicinity of the primary vertex it is often difficult to resolve the separate tracks of the particles emitted close (< 1 mrad) to the beam direction.

Simplified Glauber calculations [12] have been made of the inelastic scattering cross sections of various 200 GeV/nucleon projectile nuclei present in nuclear emulsion. The effects of nuclear correlations and excitations have been neglected so that the amplitudes correspond to the eikonal solution to the folding model approximation to the nuclear optical potential. Standard values are assumed for the proton and neutron radii of nuclei and the nucleon–nucleon total and total elastic cross section used are the measured values, 39.0 and 6.9 mb respectively. There are therefore no free parameters in the predictions of the mean free paths in emulsion displayed in Table 3. In the proton case the mean free path was estimated for 'standard' emulsion. The predicted mean free paths for both ^{16}O and ^{32}S are about 10% less than observed. This might indicate that there is a class of inelastic interactions, such as those involving little excitation of the target and/or projectile nuclei, which cannot be detected. Any loss of scanning efficiency would lead to longer path lengths. Although different loss mechanisms are present for proton and ion interactions if the results are normalized to the observed mean free path of 200 GeV protons in emulsion, namely 355 ± 8 mm [13], the predicted mean free paths for ^{16}O and ^{32}S ions become 123 and 92 mm respectively, in excellent accord with our observations shown in Table 2. The mean free paths predicted for the ion fragments, using the same scaling, are also shown in Table 3 and they agree within the errors with those found in this experiment.

The calculations also lead to estimates of the relative proportions of interactions upon hydrogen, the light (C, N, O) and heavy (Ag, Br) emulsion nuclei. The ratios change markedly with the atomic mass of the projectile, the heavier the particle the more important the interactions on the lighter targets. Some typical values are shown in Table 4.

Adamovich *et al.* [14] parametrized their ^{16}O and ^{32}S results in terms of cross sections

$$\sigma_{pA} = \sigma_1 A^{0.719}$$

$$\sigma_{A_1 A_2} = \sigma_2 \left(A_1^{0.29} + A_2^{0.29} - 1.39 \right)^2 \qquad (1)$$

with values $\sigma_1 = 38.2$ mb and $\sigma_2 = 109.2$ mb. Our data are reproduced better with $\sigma_1 = 38.7$ mb and $\sigma_2 = 116$ mb. Although the normalizations differ, the dependence of Eq. (1) on A_1,A_2 agrees with our Glauber calculation to about 1% so that the use of this parametrization would not change the relative heavy/light ratios in Table 4 in any measurable way.

3.2 Fragmentation Studies: General Features

The gross topological features observed for the interactions of ^{16}O and ^{32}S ions are displayed in Table 5. Here the forward fragments refer to those of charge 2 (^{3}He, ^{4}He) or greater ($Z \geq 3$) which make very small angles (less than about 0.1 mrad) with the direction of the original beam particle. Very similar values for 200 GeV/nucleon ^{16}O ion fragmentation to those presented in Table 5 were found by Adamovich *et al.* [15], namely, no forward fragment $29.0 \pm 1.2\%$, $Z > 2$ (presumably including those accompanied by helium emission) $36.0 \pm 1.3\%$, 1α $17.0 \pm 1.0\%$, 2α $12.1 \pm 0.8\%$, 3α $5.6 \pm 0.7\%$, and 4α $0.3 \pm 0.2\%$.

In Table 5, N_h is the number of observed target fragments, $N_h = N_b + N_g$, and their mean numbers are given for each category of event. The overall forward–backward

asymmetries, (F−B)/(F+B), observed for black prongs are consistent with the isotropic evaporation from a spallation product moving slowly forwards. The corresponding values for grey tracks, also shown in Table 5, are strongly positive since they arise predominantly from knock-on processes.

A study has also been made of the angular distributions with respect to the primary beam direction of grey tracks, those with ionization densities J_i between 1.5 and 6.0 times minimum, J_0. While these tracks are mainly due to knock-on protons (deuterons ...) there is undoubtedly some contamination due to slow pions, especially among those events with the smaller ionization values. Nevertheless the data, shown separately for ^{16}O and ^{32}S interactions in Figs. 2a and 2b respectively, are all seen to fit curves of the form $a\exp(b\cos\theta)$. The forward peaking is more pronounced in both figures for the lower values of J_i, as expected. It is also more pronounced for the ^{32}S ($b = 1.20 \pm 0.08$) than for the ^{16}O sample ($b = 1.00 \pm 0.04$). Angular distributions of this form and with similar asymmetries were found in proton-emulsion [16], ^{16}O-emulsion [17] and α-emulsion [11]. It should be noted that the angular distributions of grey tracks are almost independent of energy and centrality of the interaction [17], but several models currently used fail to reproduce the observed shape.

The N_h distributions are shown in Fig. 3 for interactions of ^{16}O and ^{32}S ions and forward-going He projectile fragments in our sample together with those from proton-emulsion interactions at (200 to 400) GeV [13]. Table 6 compares the percentages of each distribution in various intervals of N_h. Used in conjunction with Table 4, three significant trends can be noted from these data when going from proton to ^{32}S projectiles. Firstly there is a significant increase in interactions with $N_h = 0$ (much less though than the increase in ion–H interactions predicted from Table 4). Also for interactions with $N_h \leq 1$, only about 13% of them are due to interactions on H for a proton beam whereas this fraction rises to 51% for ^{32}S projectiles. Secondly there is a consistent decrease of the fraction with $5 \leq N_h \leq 15$. This feature gives rise to a shallow minimum in the distribution for $N_h \sim 10$ in the ^{32}S sample and to a plateau in the ^{16}O sample; it is completely absent in those for both the He and proton–emulsion interactions. Thirdly, interactions with $N_h > 8$ represent about 47% of p–(Ag,Br) interactions whereas this fraction rises to 63% for ^{32}S projectiles.

It is remarkable, therefore, that the average number of heavy prongs $\langle N_h \rangle$ is constant, within rather small errors (except for He) when ranging from proton– to sulphur–emulsion interactions. This is probably due to a delicate compensation. As the mass of the projectile increases, the fraction of interactions on heavy nuclei (Ag,Br) decreases but this class of collisions is likely to produce larger N_h values than do those of protons. We note that in Ref. [11], relating to 12 GeV/nucleon alpha particle interactions in emulsion, a noticeably higher multiplicity was found, namely $\langle N_h \rangle = 9.48 \pm 0.37$, but with a similar shape to the distribution. We cannot account for this discrepancy.

3.3 N_h, N_s Correlations

Of course, strong correlations are to be expected, and are indeed observed, among the degrees of disruption of the projectile ion, of the target, and of the average number $\langle N_s \rangle$ of shower particles. Figure 4 shows N_h distributions for ^{16}O and ^{32}S ion–emulsion interactions selected according to the kind of surviving forward fragments. The central and near-central interactions in which the projectile is completely disrupted, that is no projectile fragments with $Z \geq 2$ remain (No PF), show the highest degree of target frag-

mentation and also the highest number of shower particles. Increasingly more peripheral interactions show heavier or more numerous fragments of the projectile proceeding almost undisturbed along the beam direction; in these cases both $\langle N_h \rangle$ and $\langle N_s \rangle$ decrease. These correlations are clearly shown in Table 5.

For the oxygen sample, where the charges of the forward-going projectile fragments have been determined, it has been possible to examine more closely the correlations of $\langle N_h \rangle$ and $\langle N_s \rangle$ with the degree of disruption of the incident oxygen ion. These numbers are given in Table 7 as a function of $\sum Z_i$, the sum of the charges of the projectile fragments of charge two or more issuing from an interaction. Since only a subsample of events was used in this work, the numbers in this table are not directly comparable with those given in Table 5.

It is evident that, although the statistics for some of the subsamples are meagre, both pion production and evaporation energy depend primarily upon $\sum Z_i$ and not upon the detailed nature of the projectile fragmentation. More strikingly, the monotonic increases of both $\langle N_h \rangle$ and $\langle N_s \rangle$ with decreasing $\sum Z_i$ emphasize that these features are intimately linked with the centrality of the primary interaction, that is with the effective numbers of nucleon–nucleon collisions taking place. A similar correlation of $\langle N_h \rangle$ with $\sum Z_i$ was observed by Adamovich et al. [15].

3.4 Total Projectile Fragmentation Events

It is evident from Fig. 4 that the N_h distributions for the No PF class of events for ^{16}O and ^{32}S interactions are similar, both being double-peaked with a pronounced minimum for N_h values around 8. Interactions, therefore, on light and heavy nuclei appear well separated. The relative rate of this kind of interaction decreases in going from oxygen interactions, 30.0% of all events, to 16.3% for sulphur. Also, quantitatively, it is seen that 26% and 37% of ^{16}O interactions on light (C,N,O) and heavy (Ag,Br) nuclei respectively result in total projectile fragmentation. The corresponding values for ^{32}S projectiles are 11% and 23%. The considerable reduction in the comparative rates for such events from ^{16}O to ^{32}S is not unexpected. From geometrical considerations it can be seen that the probability for central and near-central interactions decreases with the increase in size of the projectile. In addition it is considerably more difficult to disrupt the heavier sulphur ion completely. In so far as one may give a pure geometrical interpretation to the total cross sections, these ratios can be fairly reproduced if it is assumed that no projectile fragment with $Z \geq 2$ can proceed undisturbed after the collision if the largest dimension within the part of the projectile outside the overlap region with the target is smaller than the diameter of an alpha particle. Thus a degree of overlap of projectile and target slightly less than, or slightly more than, the diameter of the ^{16}O and ^{32}S projectiles respectively is sufficient to result in their total fragmentation.

Central or near-central ion interactions with heavy nuclei will always involve a high number of nucleons from both nuclei. Hence a high average number $\langle N_h \rangle$ is expected with a small probability of low N_h values. The same is usually not true for collisions with the light constituents of the emulsion, so that in this case one expects to find a distribution of N_h in the whole allowed range, $0 \leq N_h \leq 8$. Indeed fits of double Gaussians to the twin-peaked N_h distributions give for ^{16}O ions $\langle N_h \rangle_{CNO} = 3.0 \pm 0.2$ ($\sigma = 2.1$), $\langle N_h \rangle_{Ag,Br} = 19.0 \pm 0.3$ ($\sigma = 6.4$) and for ^{32}S $\langle N_h \rangle_{CNO} = 2.1 \pm 0.3$ ($\sigma = 2.3$), $\langle N_h \rangle_{Ag,Br} = 19.4 \pm 0.3$ ($\sigma = 5.5$) respectively. Furthermore, the overall mean numbers of shower particles $\langle N_s \rangle$ are noticeably different when separated into the predominantly light ($N_h \leq 8$) and definitely heavy target

($N_h > 8$) samples, being 59 and 109 respectively for oxygen and 91 and 183 for sulphur interactions. This would indicate that there are about twice as many nucleon–nucleon collisions in the heavy as in the light target samples, as one would expect.

A further interesting feature is that there exist events, some 4% of those which show complete projectile fragmentation, which also exhibit no low energy target fragment emission, i.e. $N_h = 0$. For approximately 70% of the events in the oxygen sample, the number of shower particles is small, typically about 20, and each event is characterized by having several particles proceeding essentially in the beam direction. These are most probably non-interacting singly charged projectile fragments. This, together with the low multiplicities observed, indicates that these events arise almost exclusively from oxygen interactions with free protons in the emulsion, the struck proton being given sufficient energy to record a track of minimum ionization. From the expected fraction of nuclear interactions of oxygen occurring on protons (see Table 4), it is estimated that 7% of these collisions result in complete fragmentation of the oxygen nucleus. Only one of the events in the sulphur sample shows similar features, low multiplicity coupled with many spectator protons from the projectile, resulting in an efficiency of the order of 0.5% for protons to fragment the sulphur projectile completely. The overwhelming majority of the sulphur interactions and the remaining oxygen ones all exhibit much higher multiplicities, i.e. in the range 60–180, much higher than can be expected from an interaction with a single proton. Their most likely interpretation is as central interactions on the light emulsion nuclei C, N, O in which all of the target protons are struck sufficiently hard to receive relativistic velocities.

These attributions of the events are substantiated by their rapidity distributions. The emission angles, θ, of the secondary particles from these events were measured, as were those from a few central ones known to have occurred on heavy emulsion nuclei by reason of there being many low energy target fragments present.

Often in ultrarelativistic ion–nucleus experiments, the detector geometry and the events of interest are such that only particles with transverse momentum $p_T \approx p\theta \gg m$ are accepted. Consequently the geometrical variable pseudorapidity $\eta = -\ln[\tan(\theta/2)]$ is a good approximation to the kinematical variable rapidity, y, despite the lack of knowledge of the mass, m, and momentum, p, of the particle. For the events considered here, where the particles at small angles to the beam direction are largely spectator fragments from the incident ion projectile, these conditions are not however satisfied. For these the ratio of p/m is expected to be that of the beam, so that a better approximation to rapidity is given by $\tilde{y}$, where

$$y \approx \tilde{y} = \eta - \tfrac{1}{2}\ln(1 + m^2/p^2\theta^2) + \tfrac{1}{2}\ln(1 + m^2/p^2)\ , \qquad (2)$$

providing $\sin\theta \approx \theta$ and $m^2 \ll p^2$. The rapidity of an undeviated beam particle is 6.06. To accommodate the effects of measurement errors (~ 1 mrad in space angle), particles with emission angles ≤ 4 mrad have been treated as spectator fragments for this purpose. (The few produced pions within this narrow cone are expected to have a similarly high p/m ratio and do not bias the rapidity plots significantly.) Outside this angular cone, adopting an average value of 300 MeV/c for $p\theta$, $y \approx \tilde{y} \approx \eta - 0.11$.

The approximate rapidity density distributions, $\tilde{y}$, summed for different categories of events, are shown in Figs. 5a to 5e. It is at once apparent that there is a large accumulation of particles with high $\tilde{y}$ values—the projectile spectator particles—for the oxygen and sulphur interactions on free protons. It is equally clear that there is no correspondingly

large accumulation for the events -ascribed to oxygen–(C,N,O) and no evidence for such spectators in oxygen–(Ag,Br) interactions, as expected. Its absence in the latter case also serves to demonstrate that the peaks in the hydrogen samples are not an artefact of the procedure used to obtain the approximate rapidity distributions $\tilde{y}$. The peak at high $\tilde{y}$, due to the incomplete overlap of sulphur projectiles with the (C,N,O) nuclear targets, is clearly evident in Fig. 5d. On subtracting the background due to pions at high $\tilde{y}$, deduced from the fraction of such particles in the central oxygen–(Ag,Br) events of Fig. 5e, it is estimated that there are about 7, 4, 12, and 11 non-interacting protons for the O–H, O–(C,N,O), S–H, and S–(C,N,O) samples respectively.

Table 8 shows that the mean values of the rapidity distributions for each class of interaction agree with those expected, taking an effective number of participant nucleons as in Ref. [2] for interactions on heavy targets and all nucleons as participating in collisions on light nuclei. From the expected number of sulphur interactions on (C,N,O), the fraction of the events leading to complete projectile fragmentation ($\sim$ 2.4%) is roughly that expected on simple geometric grounds.

3.5 Single Alpha Emission

The distribution of N_h for those interactions in which only one helium isotope projectile fragment remains shows for ^{32}S ion collisions a similar double-peaked behaviour to that observed for complete projectile disruption with $\langle N_h \rangle_{CNO} = 2.7 \pm 0.4$ ($\sigma = 2.2$), $\langle N_h \rangle_{Ag,Br} = 18.9 \pm 0.5$ ($\sigma = 4.9$). There is a ratio 1.4 : 1 between interactions on heavy (Ag,Br) and light (C, N, O) nuclei and this is approximately the same ratio as for all interactions as predicted in Table 4. The N_h distribution for this class of events for oxygen interactions does not exhibit the double-peaked feature. However any reasonable continuation of the distribution for $N_h > 8$, arising solely from interactions on heavy nuclei, to $N_h \leq 8$ indicates that the ratio of interactions on heavy and light nuclei is also similar to that for the whole sample. The mean numbers of shower particles are again well correlated with N_h, being 31 and 68 for oxygen and 68 and 121 for sulphur interactions for samples with $N_h \leq 8$ and $N_h > 8$ respectively.

For more peripheral interactions, those in which two or more He isotopes and/or a heavier fragment continue undisturbed, it is more difficult to separate interactions on heavy and light nuclei as shown in Fig. 4.

4. CONCLUSIONS

The mean free paths for both primary ^{16}O and ^{32}S ions as well as projectile fragments of various charges produced by an initial oxygen beam have been measured. Whereas the statistics are in many cases poor and the isotopic constitutions are not known, there is reasonable agreement with expectation.

Both the oxygen and sulphur results show the same general features, the greater the disruption of the projectile nucleus, the greater that of the target and the higher the number of shower particles produced. The measurement of the charges of the projectile fragments from oxygen interactions has enabled these correlations to be clearly demonstrated.

The low energy fragments (black tracks) are shown to arise predominantly from isotropic evaporation from the target nuclei, whereas the grey tracks are strongly peaked forwards, as is to be expected if arising from knock-on processes. The angular distributions of grey tracks, obtained in the present and previous studies, seem to be almost independent

of the energy or nature of the projectile, and even of the centrality of the collision; however, several models of nuclear interactions currently used fail to reproduce the observed shape.

Although the mean numbers of heavy prongs, $\langle N_h \rangle$, are similar for interactions in emulsion produced by projectiles ranging from protons to ^{32}S ions, the shapes of the distributions are different. This apparent anomaly is explained in part by the more peripheral nature of ion interactions and also by the growing importance of the contribution of light target nuclei in the emulsion, especially hydrogen, to the cross section with increasing projectile mass. The distributions also show that with increasing projectile size it becomes more easy to discern the contributions from collisions with light and heavy nuclei. Furthermore for a given ion projectile, the shapes of the N_h distributions of subsamples selected according to the type and/or number of forward-going fragments are very different.

A study of the N_h distribution for those events in which the primary oxygen and sulphur ions are completely disrupted indicates that the contribution from light nuclear targets is high. For the particular subset of these interactions in which there is no apparent low energy target fragmentation ($N_h = 0$), the multiplicities and the rapidity distributions demonstrate that for the oxygen sample these events arise dominantly from interactions on free protons, whereas for sulphur they are almost exclusively from C, N, O targets. The probability for oxygen projectile nuclei to overlap completely light target nuclei and the collision of a sulphur projectile with a proton to result in its complete fragmentation must both be small, and this has been borne out by the observations. On the other hand the rapidity distributions of the shower particles rule out this subsample as arising from electromagnetic or diffractive dissociation processes.

Acknowledgements

It is a pleasure to acknowledge the excellent performance of the CERN PS and SPS, and the enthusiastic work of the related staffs. We are also very grateful to our scanning teams for their patience and efficiency.

Support from the Mitsubishi Foundation, from the Japan Society for the Promotion of Science, and from the Monbusho International Scientific Research Program is greatly appreciated.

REFERENCES

[1] T. Åkesson *et al.*, Z. Phys. **C38** (1988) 383; Phys. Lett. **B214** (1988) 295.
[2] T. Åkesson *et al.*, Nucl. Phys. **B342** (1990) 279.
[3] N. Ardito *et al.*, Europhys. Lett. **6** (1988) 131.
[4] W.H. Barkas, *Nuclear Research Emulsions* (Academic Press, London & New York, 1963), Vol. 1, p. 70.
[5] G. Baroni *et al.*, Nucl. Phys. **A516** (1990) 673.
[6] M.I. Adamovich *et al.*, Phys. Lett. **223B** (1989) 262.
[7] L.M. Barbier *et al.*, Phys. Rev. Lett. **60** (1988) 405.
[8] K. Sengupta, G. Singh and P.L. Jain, Phys. Lett. **222B** (1989) 301.
[9] G. Singh, K. Sengupta and P.L. Jain, Phys. Rev. **C42** (1990) 1757.
[10] K. Sengupta, G. Singh, T. Ritter and P.L. Jain, Europhys. Lett. **8** (1989) 15.
[11] V.S. Shukla *et al.*, Mod. Phys. Lett. **A18** (1988) 1753.
[12] R.J. Glauber, in *Lectures in Theoretical Physics*, Ed. W.E. Brittin (Interscience, New York, 1959), Vol. 1, p. 315.
[13] I. Stenlund and I. Otterlund, Nucl. Phys. **B198** (1982) 407.
[14] M.I. Adamovich *et al.*, Mod. Phys. Lett. **A5** (1990) 164.
[15] M.I. Adamovich *et al.*, Phys. Rev. **C40** (1989) 66.
[16] I. Otterlund *et al.*, Nucl. Phys. **B142** (1978) 445.
[17] M.I. Adamovich *et al.*, Phys. Lett. **230B** (1989) 175.

Table 1: Composition of emulsions

Element	Standard (10^{20} atoms/cm^3)	Fuji (10^{20} atoms/cm^3)
H	322	350
C	138	127
N	32	29
O	95	114
Br	101	93
Ag	101	93

Table 2: Results of following primary ^{16}O, ^{32}S, and secondary (+ tertiary, ...) projectile fragments. Shown separately are the numbers we ascribe to electromagnetic dissociation (EMD) and other inelastic nuclear processes.

Projectile fragment	Number followed	Total path (m)	No. inelastic interactions	No. EMD	$\lambda_{\text{inel}} \pm \Delta\lambda_{\text{inel}}$ (mm)	$\lambda_{\text{EMD}} \pm \Delta\lambda_{\text{EMD}}$ (mm)
He	1909	91.0	399	13	228 ± 11	7000 ± 1900
Li	133	6.4	38	2	167 ± 27	3200 ± 2200
Be	139	6.1	40	6	153 ± 24	1000 ± 400
B	193	8.4	65	4	129 ± 16	2100 ± 1000
C	408	17.9	125	13	143 ± 13	1400 ± 400
N	460	20.2	161	14	126 ± 10	1400 ± 400
O	13395	349.4	2924	365	120 ± 2	960 ± 50
S	8693	214.4	2319	515	92 ± 2	420 ± 20

Table 3: Glauber calculations of σ_{inel} of various 200 GeV/nucleon projectile nuclei upon target emulsion nuclei

Projectile nucleus	σ_{inel} (mb) Target nucleus						λ_{inel} (mm)	λ_{inel} (mm) Renormalized
	H	C	N	O	Br	Ag		
^{1}H	32	253	278	318	1004	1266	319[a]	355[a]
^{3}He	87	505	542	604	1520	1847	203	226
^{4}He	100	533	568	634	1562	1891	195	217
^{6}Li	168	775	822	901	2006	2384	144	161
^{9}Be	220	874	922	1008	2159	2552	130	149
^{11}B	241	896	942	1030	2187	2584	127	142
^{12}C	253	919	965	1055	2224	2624	124	138
^{14}N	278	965	1012	1104	2297	2706	119	132
^{16}O	318	1055	1104	1201	2442	2861	110	123
^{32}S	523	1448	1508	1623	3058	3517	83	92

[a] Computed for standard emulsion.

Table 4: Relative proportions of interactions upon light and heavy emulsion nuclei according to the Glauber model

Projectile nucleus	Target nucleus		
	H (%)	C, N, O (%)	Ag, Br (%)
^{1}H	3.3	23.6	73.1
^{4}He	6.9	30.5	62.6
^{6}Li	8.5	32.5	59.0
^{9}Be	10.0	32.9	57.1
^{12}C	11.0	32.9	56.1
^{16}O	12.3	33.4	54.4
^{32}S	15.2	34.2	50.6

Table 5: Topological features observed for ^{16}O and ^{32}S ion interactions

Beam	^{16}O				^{32}S			
Number of nuclear events	2924				2319			
Total $\langle N_h \rangle$	7.56 ± 0.15				7.42 ± 0.17			
Total $\langle N_s \rangle$	44.0 ± 1.5				56.0 ± 1.2			
F/B asymmetry black tracks	0.077 ± 0.009				0.099 ± 0.010			
F/B asymmetry grey tracks	0.386 ± 0.009				0.403 ± 0.011			
Projectile fragments	No.	%	$\langle N_h \rangle$	$\langle N_s \rangle$	No.	%	$\langle N_h \rangle$	$\langle N_s \rangle$
None	878	30.0	13.8	93.1	379	16.3	14.9	155.9
1α	502	17.2	8.2	45.7	240	10.4	12.1	102.3
2α	325	11.1	5.1	23.9	157	6.8	9.1	72.5
3α	171	5.9	3.4	13.3	108	4.7	7.3	47.8
4α	9	0.3	2.4	4.2	54	2.3	6.2	32.1
5α	–	–	–	–	22	1.0	6.6	34.0
6α	–	–	–	–	6	0.3	2.5	19.5
1 $Z \geq 3$ no α	854	29.2	3.6	13.6	796	34.3	4.0	16.3
1 $Z \geq 3$ + α's	185	6.3	2.9	11.6	530	22.9	4.9	24.9
2, 3 $Z \geq 3$	–	–	–	–	27	1.2	5.3	30.0

Table 6: Percentage distribution between various intervals of N_h
for H, He, ^{16}O, and ^{32}S projectiles.
The proton data, taken from Ref. [12], refer to the energy range 200–400 GeV.

	N_h						
	0	1	2–4	5–8	9–15	≥ 16	$\langle N_h \rangle$
^{1}H	14.7±0.4	10.8±0.3	22.3±0.5	18.0±0.4	16.8±0.4	17.4±0.4	7.63±0.08
He	18.7±2.1	7.6±1.4	25.6±2.5	18.7±2.1	15.3±1.9	14.0±1.9	6.74±0.33
^{16}O	18.4±0.8	9.3±0.6	24.9±0.9	14.5±0.7	13.1±0.7	19.8±0.8	7.56±0.15
^{32}S	19.6±0.9	10.0±0.7	24.5±1.0	13.9±0.8	11.6±0.7	20.3±1.0	7.42±0.17

Table 7: $\langle N_h \rangle$ and $\langle N_s \rangle$ as a function of $\sum Z_i$ for incident ^{16}O ions

$\sum Z_i$		No. of interactions	$\langle N_h \rangle$	$\langle N_s \rangle$
8	O	16	1.7	4.9
	Cα	26	2.0	5.4
	Be$\alpha\alpha$	3	1.3	7.3
	$\alpha\alpha\alpha\alpha$	7	3.0	4.9
	Total	52	2.0	5.3
7	N	247	3.0	9.2
	Bα	27	2.7	9.1
	Li$\alpha\alpha$	10	1.4	9.2
	Total	284	2.9	9.2
6	C	252	3.6	13.1
	Beα	39	2.8	14.8
	$\alpha\alpha\alpha$	139	3.5	13.3
	Total	430	3.5	13.3
5	B	88	3.7	15.9
	Liα	42	3.7	14.8
	Total	130	3.7	15.5
4	Be	55	5.0	24.6
	$\alpha\alpha$	261	4.8	23.9
	Total	316	4.8	24.0
3	Li	39	6.3	26.4
2	α	409	8.0	45.7
0	–	711	13.2	93.1

Table 8: Expected and observed mean rapidity values

Projectile nucleus		Target nucleus		
		H	C, N, O	Ag, Br
^{16}O	expected	4.4	3.0 - 3.2	2.5
	observed	4.4	3.3	2.8
^{32}S	expected	4.8	3.4 - 3.5	2.6
	observed	4.7	3.6	–

Figure captions

Figure 1: Charge distribution of secondary projectile fragments from a subsample of ^{16}O interactions as determined by δ-ray density measurement.

Figure 2: Angular distribution of 'grey' tracks having ionization densities between 1.5 and 6.0 times minimum, a) from ^{16}O interactions, b) from ^{32}S interactions. The fitted curves are of the form $a\,e^{b\,\cos\theta}$.

Figure 3: Distributions of the number N_h of target fragments from interactions of ^{16}O and ^{32}S ions and forward-going He projectile fragments in our sample, together with those from proton–emulsion interactions at (200 to 400) GeV [13].

Figure 4: Distributions of N_h for ^{16}O and ^{32}S ion–emulsion interactions selected according to the types of surviving forward fragments.

Figure 5: Approximate rapidity-density distributions ($\rho = N_{ev}^{-1}dN/dy$) determined using the method described in the text, a) ^{16}O–H; b) ^{16}O–C,N,O; c) ^{32}S–H; d) ^{32}S–C,N,O; e) ^{16}O–Ag,Br central interactions.

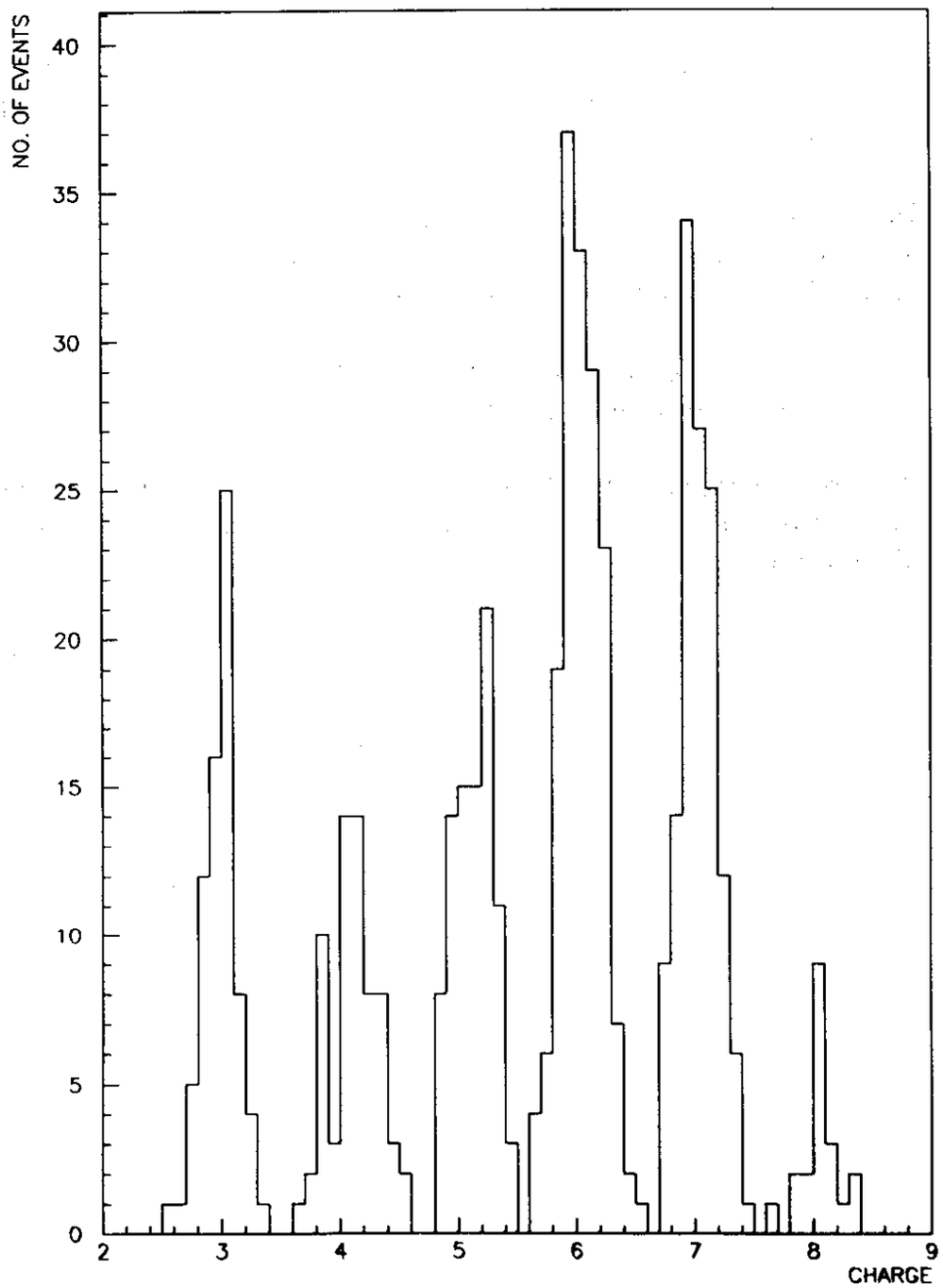

Fig. 1

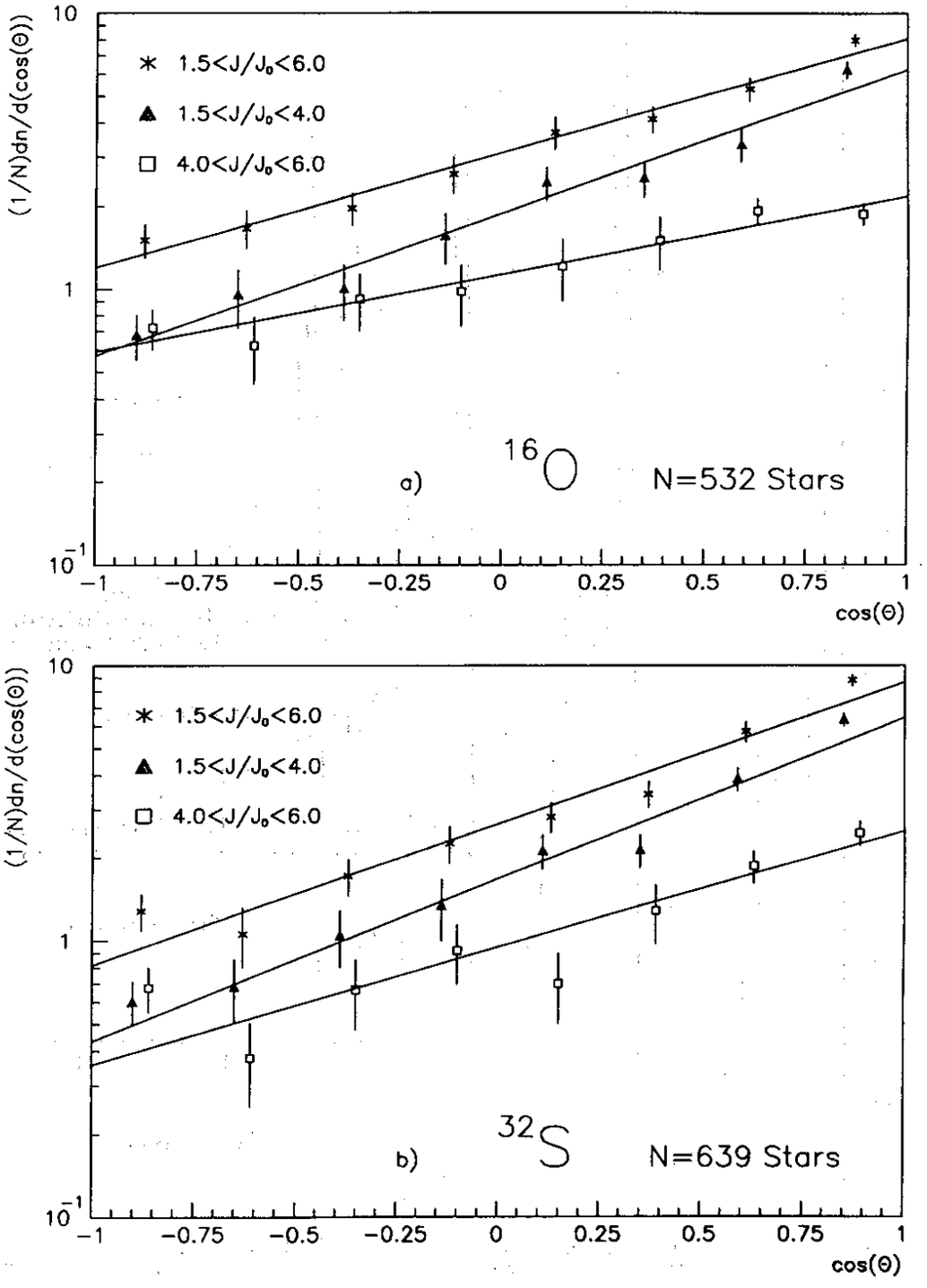
(1/N)dn/d(cos(Θ))
10
1
10^{-1}
* 1.5<J/J₀<6.0
▲ 1.5<J/J₀<4.0
□ 4.0<J/J₀<6.0
a) ^{16}O N=532 Stars
−1 −0.75 −0.5 −0.25 0 0.25 0.5 0.75 1
cos(Θ)
(1/N)dn/d(cos(Θ))
10
1
10^{-1}
* 1.5<J/J₀<6.0
▲ 1.5<J/J₀<4.0
□ 4.0<J/J₀<6.0
b) ^{32}S N=639 Stars
−1 −0.75 −0.5 −0.25 0 0.25 0.5 0.75 1
cos(Θ)

Fig. 2

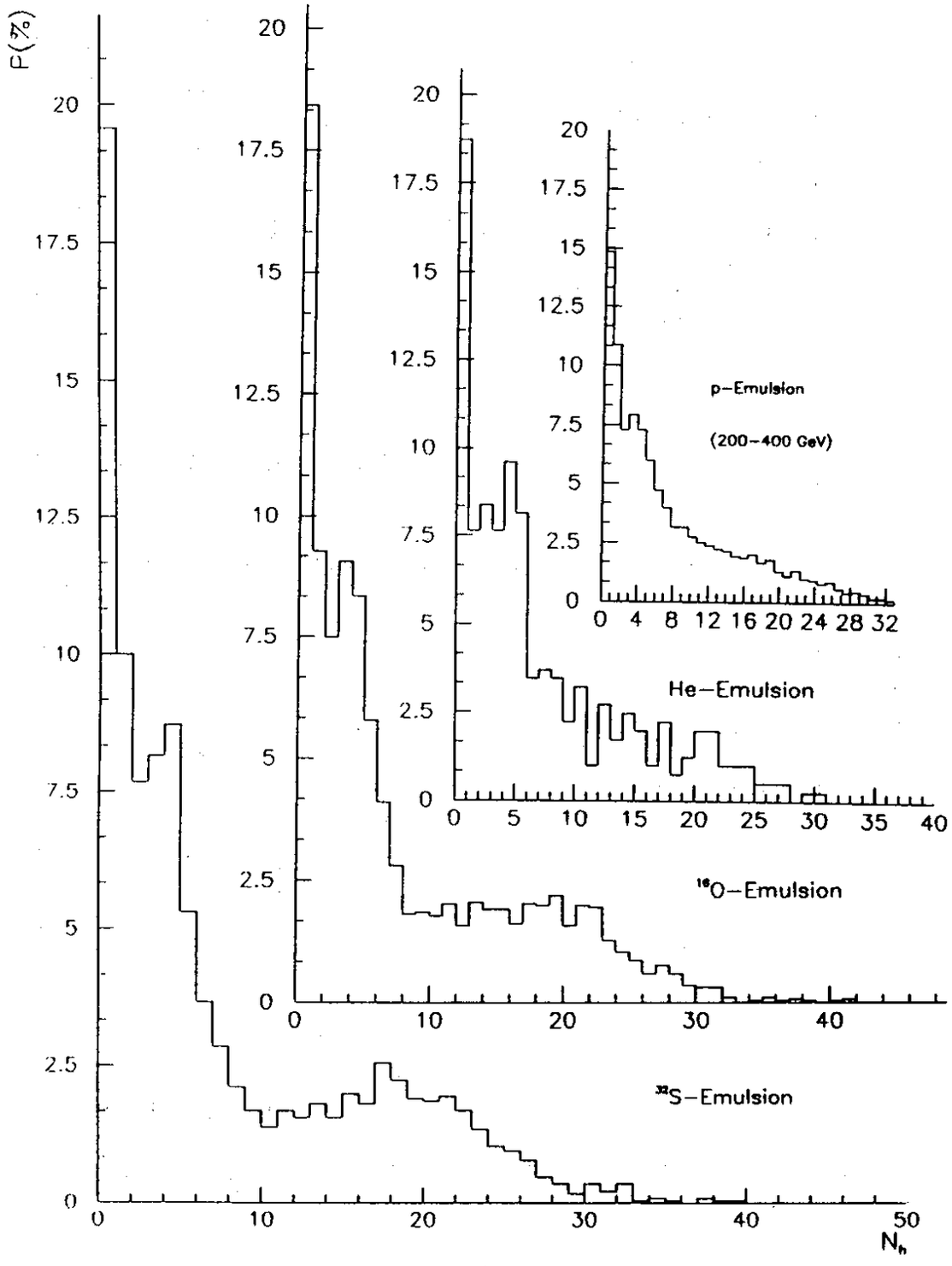
P(%)
p–Emulsion
(200–400 GeV)
He–Emulsion
^{16}O–Emulsion
^{32}S–Emulsion
N_h

Fig. 3

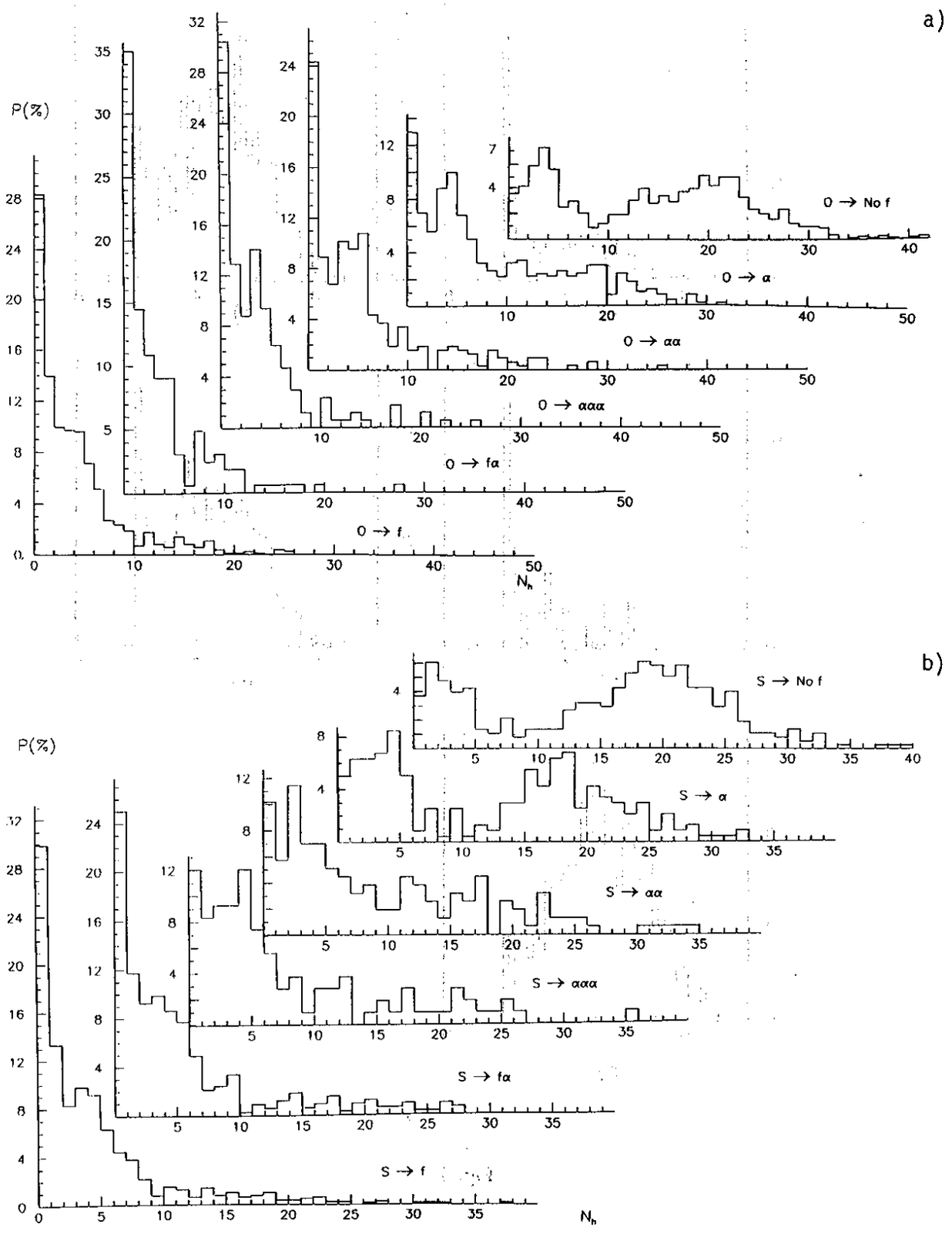

Fig. 4

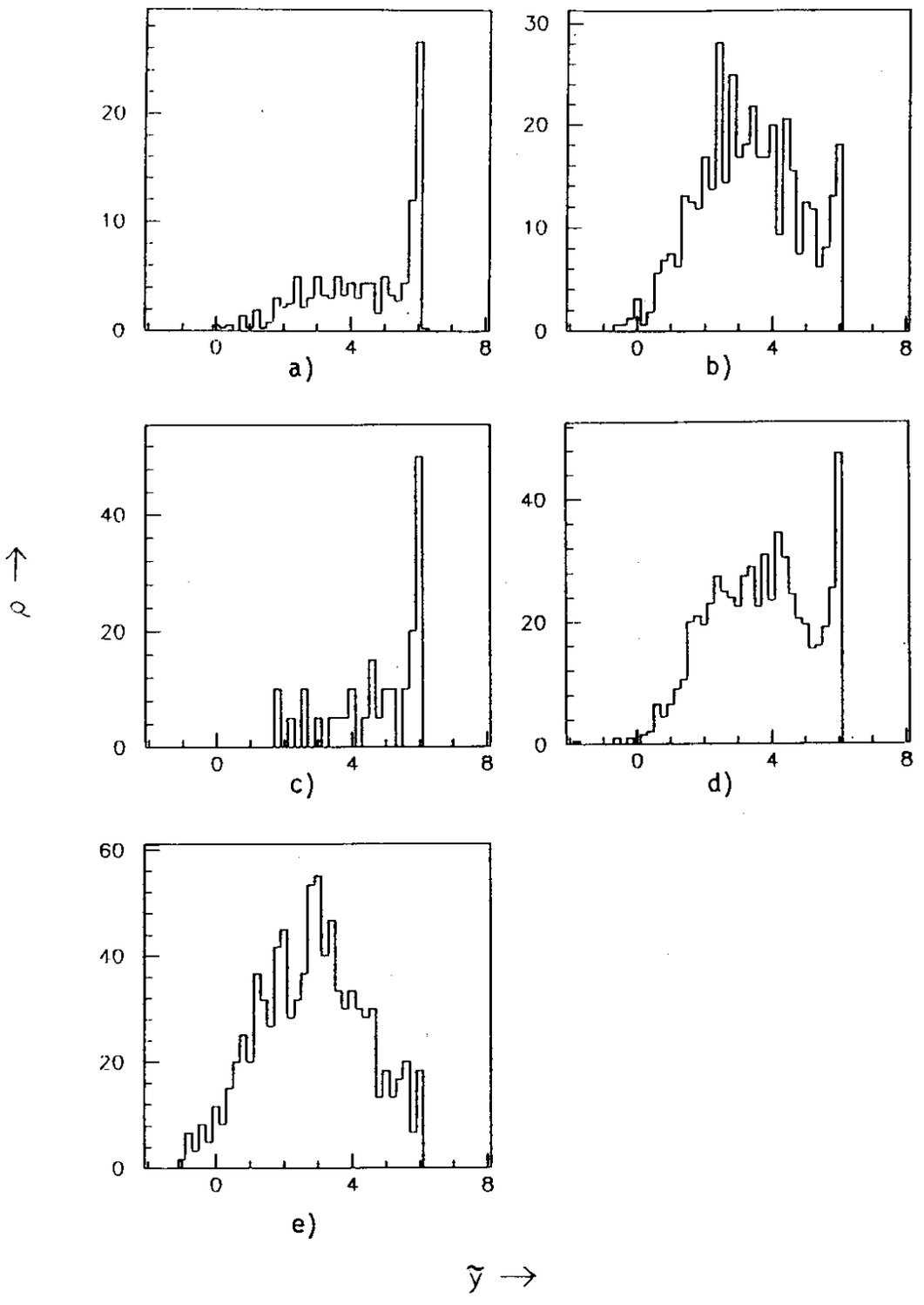

Fig. 5

Imprimé au CERN. Prix : 0.70 Fr.